Laminar burning velocities and lean flammability limits of H2/CO/CH4/CO2/air mixtures associated with gases vented out Li-ion

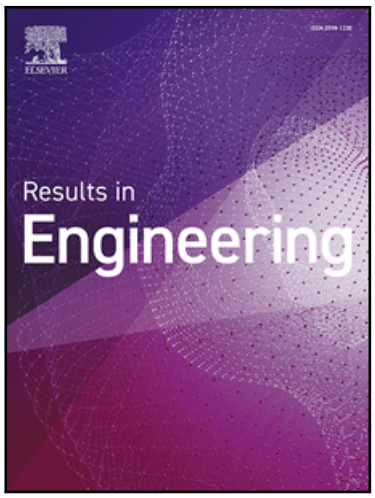

Laminar burning velocities and lean flammability limits of $H_2/CO/CH_4/CO_2$/air mixtures associated with gases vented out Li-ion batteries after thermal runaway

Andrei N. Lipatnikov

PII: S2590-1230(25)04320-8
DOI: https://doi.org/10.1016/j.rineng.2025.108274
Reference: RINENG 108274

To appear in: *Results in Engineering*

Received date: 3 September 2025
Revised date: 31 October 2025
Accepted date: 17 November 2025

Please cite this article as: Andrei N. Lipatnikov , Laminar burning velocities and lean flammability limits of $H_2/CO/CH_4/CO_2$/air mixtures associated with gases vented out Li-ion batteries after thermal runaway, *Results in Engineering* (2025), doi: https://doi.org/10.1016/j.rineng.2025.108274

Highlights

- Laminar flame speeds are computed for a wide set of H_2/CO/CO_2/CH_4/air mixtures
- Weak influence of CO concentration on lean flammability limit of H_2/CO/air mixtures
- In H_2/CO/CO_2/CH_4 blends, methane can mitigate fire risk better than inert CO_2
- For H_2/CO/CO_2/CH_4/air mixtures with large volume fraction of CO_2 there is fire risk

Laminar burning velocities and lean flammability limits of H_2/CO/CH_4/CO_2/air mixtures associated with gases vented out Li-ion batteries after thermal runaway

Andrei N. Lipatnikov*
Department of Mechanics and Maritime Sciences, Chalmers University of Technology, Gothenburg, 412 96, Sweden

Abstract

To explore major combustion characteristics of mixtures relevant to gases vented out Li-ion batteries, complex-chemistry simulations of laminar flames are performed for a wide range of H_2/CO/CO_2/CH_4/air mixtures by varying equivalence ratio and mole fractions of these species. The simulations are done for different temperatures of unburned reactants, using three state-of-the-art chemical mechanisms and multicomponent diffusion model with Soret effect. The focus of the study is placed on the influence of concentrations of CO, CO_2, and CH_4 on the computed laminar flame speeds S_L and a surrogate of lean flammability limit, i.e., equivalence ratio ϕ^* associated with a small speed $S_L(\phi^*) = 5$ cm/s. Results show that, first, both $S_L(\phi)$ in lean mixtures and ϕ^* depend weakly on mole fraction of CO in H_2/CO blends. Second, an increase in ϕ^* and a decrease in $S_L(\phi)$ in lean mixtures are more (less) pronounced when adding CH_4 (CO_2, respectively) to H_2/CO blends. Accordingly, under certain conditions, fuel can reduce $S_L(\phi)$ more than diluent. These observations are attributed to a larger (smaller) increase in the mole fraction of inert species when adding CH_4 (CO_2, respectively) to H_2/CO blends but retaining the same (low) equivalence ratio. Finally, results show that a large volume fraction of CO_2 in gases vented out a battery does not exclude fire risks.

Keywords: Li-ion battery, fire risk, flammable jets, laminar flame speed, lean flammability limit, numerical simulations

1. Introduction

Li-Ion Battery (LIB) technology is a promising tool for sustainable development of clean and efficient power sources that utilize renewable energy and operate without contributing to the accumulation of greenhouse gases in the atmosphere. High power density, light weight and a long lifespan are important advantages of LIBs [1-5], which promote a rapid growth of the number of LIBs used in various sectors worldwide, ranging from small-scale applications such as cell phones and laptops to large-scale applications such as vehicles, aircraft, and ships. However, the high energy density is a hazard also. For instance, leakage of flammable electrolytes such as diethyl carbonate or dimethyl carbonate after damage of LIB poses fire risk. Moreover, LIB failures due to thermal abuse (overheat), electrical abuse (overcharging or discharging), internal short-circuit, or mechanical abuse (e.g., car crash) can trigger internal exothermic reactions within the LIB cell. Such reactions build flammable gases and increase the cell temperature, thus causing the cell to undergo thermal runaway [5-10]. Subsequently, preheated flammable gases can be released into the atmosphere and mixed with the air, followed by ignition and appearance of a jet fire or even explosion, which poses a significant risk to surroundings.

Due to the rapid growth of the number of LIBs worldwide, the number of fire incidents caused by failures of such batteries is also increased, e.g., see Table 2 in Ref. [5] or Table 3 in Ref. [10], thus, calling for intensifying research into LIB fire safety. As stated in a recent review article by Wang et al. [10], "*safety issue is still the main obstacle to the usage of LIBs in large scale applications, such as EVs and energy storage systems*", but "*comprehensive modeling of the flames produced by the materials ejected from LIB has not been performed to date*".

*Corresponding author
E-mail address: lipatn@chalmers.se

These safety issues triggered research into jet fires associated with LIBs [11,12] and, in particular, into major combustion characteristics of gases vented out a LIB after thermal runaway. Such research deals with two different groups of fuels, i.e., (i) liquid carbonate esters used as electrolyte solvents in LIBs, e.g., see Refs. [13-15] and references quoted therein, and (ii) mixtures of light molecules such H_2, CO, CO_2, CH_4, C_2H_4, etc. [16,17]. In the former case, a fire may occur due to leakage of the solvents from a destroyed LIB, followed by the solvent evaporation and ignition. In the latter case, hot flammable gases are vented out a damaged LIB after thermal runaway, with the solvent molecules being decomposed into simpler molecules during the thermal runaway inside the battery. Typically, these two types of fires (liquid solvents or hot gases) do not appear simultaneously and are explored separately.

The present work is solely restricted to the latter (gaseous) mixtures. For them, two major combustion characteristics are in the research focus. These are (ii.a) ignition delay time and explosion limits [18,19] and (ii.b) laminar flame speed and flammability limits [20,21]. The present work is solely restricted to item (ii.b) and to numerical research.

Currently, advanced tools for computing laminar flame speeds of various fuel blends with the air are routinely used, as reviewed elsewhere [22]. These tools involve well validated (under room conditions) chemical mechanisms, e.g., [23-25], various computational software [26-28], molecular transport models [29] and transport property databases [30,31], a widely adopted thermodynamic property database [27], models of radiative heat transfer from flames, e.g., [19], etc. Accordingly, advanced simulations of laminar flame speeds and flammability limits are feasible for various fuel blends and such numerical studies were already performed for gases vented out LIBs after thermal runaway [18,19]. For instance, Henriksen et al. [18] investigated three H_2/CO/CO_2/CH_4/C_2H_4/C_2H_6/air mixtures and Yu et al. [19] explored burning of a single blend of H_2, CO, CH_4, and C_2H_4 diluted with various amounts of CO_2, H_2O, or N_2.

While the cited studies demonstrated predictive capabilities of state-of-the-art research tools and delivered valuable quantitative data, these results were restricted to few combinations of concentrations of hydrogen, carbon oxide, and small hydrocarbons in a fuel blend. Since mole fractions of H_2, CO, CH_4, CO_2, and other molecules vary in wide ranges in gases vented out different batteries under different States Of Charge (SOCs) [11,16-18,32-37], there is also a need for a systematic qualitative study of major trends associated with the influence of fractions of various species in such fuel blends on laminar flame speeds and flammability limits. The present work aims at performing such a qualitative study for many H_2/CO/CO_2/CH_4/air mixtures by separately varying mole fraction of each molecule in a wide range of concentrations, associated with compositions of gases vented out LIBs after thermal runaway.

In the next section, background is summarized. The research method is briefly presented in section 3. Computed results are discussed in section 4, followed by conclusions.

2. Background

Unperturbed laminar flame speed S_L is one of the major fundamental characteristics of a reacting gaseous mixture. It is the speed of a planar, one-dimensional, adiabatic flame, whose internal structure is stationary, with respect to the upstream stationary, one-dimensional, and spatially uniform flow of unburned reactants [38]. Under these simplest conditions, the speed S_L is solely controlled by mixture composition, pressure, and temperature. This fundamental speed is (i) a target for validation of chemical mechanisms of combustion of various fuels, as reviewed elsewhere [22], and (ii) the key input parameter for various models of (partially) premixed turbulent burning [39,40], e.g., turbulent combustion rate is increased by S_L, as reviewed elsewhere [41]. To run numerical simulations of turbulent burning of gaseous jets vented out LIBs [11,12], values of S_L are typically required.

This laminar flame speed depends on many factors such as burning temperature T_{ad}, i.e., temperature of adiabatic combustion products in equilibrium state, molecular transport coefficients, combustion chemistry, pressure, etc. According to the classical theory [38], T_{ad} is the dominant factor, because (i) the major chain-branching and chain-propagating reactions are localized to narrow zones where the local temperature T is smaller than but sufficiently close to T_{ad}, (ii) the reaction rates depend exponentially on Θ/T, with (iii) the activation temperature Θ being typically high, i.e., $\Theta/T_{ad} \gg 1$. On the contrary, dependence of S_L on pressure, molecular transport coefficients, or details of a reaction mechanism is much weaker than the exponential one [38].

If reactant temperature is kept constant, the burning temperature T_{ad} depends on heats of formation of fuel and oxidant (oxygen in the air), heat capacities of various species, but is mainly controlled by concentration of inert diluents in the mixture, which do not contribute directly to heat release, but consume heat released in chemical reactions between active species. Typically, T_{ad} is the highest in near-stoichiometric mixtures where all fuel and all oxygen are almost completely consumed [38,42]. In lean mixtures, a part of oxygen, which is an excess component, is not consumed, but acts as an inert diluent. Accordingly, the leaner a lean mixture, the lower T_{ad}. In rich mixtures, concentration of oxygen is not sufficient for the entire fuel to be fully consumed. Consequently, some products of incomplete combustion mimic an inert diluent. Therefore, the richer a rich mixture, the lower T_{ad}.

If a mixture is too lean or too rich, T_{ad} is too low for chain-branching and chain-propagating reactions whose rates depend exponentially on Θ/T to dominate termolecular radical recombination (chain-terminating) reactions whose rates are weakly sensitive to temperature [43]. Moreover, heat release can be insufficient to overcome even small heat losses [38]. Accordingly, flame propagation is not possible in so lean or so rich mixtures. Lean (rich) flammability limit is the lowest (highest) concentration of fuel in the lean (rich) mixture that can still burn. Contrary to S_L and T_{ad}, flammability limits are not fundamental mixture characteristics, but depend on many other factors such heat losses, buoyancy, flow non-uniformities, differences between molecular diffusivities of major reactants, flame configuration and stretch rate, etc. [42,44]. Since any of these factors can play an important role depending on conditions, quantitative prediction of flammability limits is a feasible [21], but difficult task, which requires expensive multi-dimensional numerical simulations of complex-chemistry, non-adiabatic flames propagating in non-uniform flows. Accordingly, flammability limits are often associated with a small reference value of S_L, e.g., $S_L^* = 5$ cm/s [45,46]. Since the present study aims solely at exploring qualitative trends, this simplest method will be used in the following. Moreover, the focus will be placed on lean mixtures, which are crucial for assessing explosion risks. Indeed, if reactants are very rich (beyond rich flammability limit), subsequent mixing with surrounding air can make conditions flammable later. If reactants are very lean, such mixing will make the reactants leaner.

Since S_L is primarily controlled by T_{ad}, which in its turn is controlled by concentration of inert species, it is plausible to highlight this concentration when discussing the influence of mole fractions of various species in H_2/CO/CO_2/CH_4 fuel blend on S_L. Accordingly, let's consider the following generic reaction

$$\phi(\mathrm{H_2} + \alpha\mathrm{CO} + \beta\mathrm{CH_4} + \gamma\mathrm{CO_2}) + \left(\frac{1}{2} + \frac{\alpha}{2} + 2\beta\right)(\mathrm{O_2} + 3.76\mathrm{N_2})$$

$$= \phi(1 + 2\beta)\mathrm{H_2O} + \phi(\alpha + \beta + \gamma)\mathrm{CO_2} + (1 - \phi)\left(\frac{1}{2} + \frac{\alpha}{2} + 2\beta\right)\mathrm{O_2} + 3.76\left(\frac{1}{2} + \frac{\alpha}{2} + 2\beta\right)\mathrm{N_2},$$

where $\phi < 1$ is equivalence ratio, $1/2 + \alpha/2 + 2\beta$ is the stoichiometric ratio, and number 3.76 stays for the air. Here, complete combustion is assumed (i.e., small concentrations of CO and other species in products are neglected). Since inert species involve not only CO_2 and N_2, but also a part of oxygen, i.e., $(1 - \phi)(1/2 + \alpha/2 + 2\beta)$ molecules of O_2, the total mole fraction of inert species is equal to

$$X_{in} = \frac{\phi\gamma + (1 - \phi)\left(\frac{1}{2} + \frac{\alpha}{2} + 2\beta\right) + 3.76\left(\frac{1}{2} + \frac{\alpha}{2} + 2\beta\right)}{\phi(1 + \alpha + \beta + \gamma) + 4.76\left(\frac{1}{2} + \frac{\alpha}{2} + 2\beta\right)}. \quad (1)$$

If one or two species in H_2/CO/CO_2/CH_4 fuel blend are absent, mole fractions of inert species can be calculated using formulas reported in Table 1.

Table 1
Mole fractions of inert species in various lean H_2/CO/CO_2/CH_4/air mixtures

Fuel blend	Coefficients	X_{in}
H_2/CO	$\beta = \gamma = 0$	$\dfrac{-\frac{\phi}{2} + 2.38}{\phi + 2.38}$
H_2/CH_4	$\alpha = \gamma = 0$	$\dfrac{-\frac{\phi}{2} + 2.38}{\phi - \frac{3\phi}{\beta^{-1} + 4} + 2.38}$
H_2/CO_2	$\alpha = \beta = 0$	$1 - \dfrac{\frac{3}{2}\phi}{\phi(1+\gamma) + 2.38}$
H_2/CO/CH_4	$\gamma = 0$	$\dfrac{-\frac{\phi}{2} + 2.38}{\phi - \frac{3\phi}{(1+\alpha)/\beta + 4} + 2.38}$
H_2/CO/CO_2	$\beta = 0$	$1 - \dfrac{3\phi}{2\left(\phi + \frac{\phi\gamma}{1+\alpha} + 2.38\right)}$

3. Method

3.1. Numerical simulations

Stationary, one-dimensional, planar, adiabatic laminar premixed flames are numerically simulated running PREMIX module [29] of CHEMKIN-II software package [26]. The flames are described with common transport equations for mass, momentum, energy, and species concentrations [29] and by the ideal gas state equation. In the studied case, governing partial differential transport equations degenerate to a set of non-linear ordinary differential equations, which are iteratively solved. Molecular mass and heat transfer is described adopting multicomponent transport model [29], with Soret effect being also considered, because it is known to substantially affect speeds of hydrogen-air or syngas-air laminar flames [47-50]. The numerical grid is automatically refined when a normalized slope of computed variables (parameter GRAD in PREMIX module) exceeds 0.02 at any point, with weak sensitivity of computed results to variations in this threshold being checked.

For simple fuel molecules like H_2, CO, or CH_4, there are dozens of advanced chemical mechanisms, as reviewed elsewhere [22,51-53]. Since they were validated using the same experimental data, these mechanisms yield close values of laminar flame speeds, e.g., see Fig. 34 in Ref. [22] as a typical example. While there are small quantitative differences between values of S_L, computed using different mechanisms, such differences are often comparable with measurement errors or scatter of experimental data. Moreover, these quantitative differences are smaller in lean mixtures, with the qualitative trends being the same. Accordingly, results presented in the following were obtained adopting three of such mechanisms [23-25], which were tested in many papers. Specifically, GRI mechanism [23] is the earliest and most widely used one, especially for methane, e.g., see Figs. 34-45 in Ref. [22] or Fig. 8 in Ref. [53]. Results of validation of this mechanism against data on S_L measured in CH_4-air, H_2/CO/CO_2-air, or H_2/CO/CH_4-air mixtures, can be found, e.g., in Refs. [54], [55], and [56], respectively. This mechanism was also validated for four mixtures associated with gases vented out LIBs [20]. It is worth noting, however, that performance of GRI mechanism is worse for H_2-air mixtures [57]. The two other mechanisms are more modern. Princeton mechanism [24] was particularly well validated for H_2/CO-air flames [58-61]. It was also validated for few H_2/CO/CH_4-air mixtures [62], but the present author is not aware of results of testing this mechanism against data on S_L, obtained from more complicated mixtures that are vent out LIBs. San Diego mechanism [25] was validated for H_2-air [52,57,62], H_2/CO-air [63], or CH_4-air [22,53] mixtures, was recently applied to modeling explosion limits of NCA battery vent gas [19], and was validated for four mixtures associated with gases vented out LIBs [20].

Results of the present simulations are used not only for computing the flame speed† S_L, but also for evaluating thermal laminar flame thickness

$$\delta_L = \frac{\max\{|\nabla T|\}}{(T_{ad} - T_u)}. \quad (2)$$

Here, the maximum temperature gradient is taken along the distance normal to the flame and T_u designates unburned gas temperature. This flame thickness is another fundamental characteristic of a flammable mixture [38] and is of interest, because a typical gaseous jet fire occurs in a turbulent flow and turbulent burning rate is increased not only with increasing S_L but also with decreasing δ_L, as reviewed elsewhere [41], see also a recent paper by Wang et al. [64]. Accordingly, this thickness is another important input parameter for modeling turbulent combustion [39,40,65,66].

3.2. Conditions

Since the present study aims at qualitatively exploring the influence of concentrations of various species in H_2/CO/CO_2/CH_4 fuel blend on S_L, δ_L, and lean flammability limit, four groups of cases were simulated. Within each group, (i) T_u was set equal to 300, 400, 500, or 600 K, (ii) pressure was atmospheric, and (iii) the equivalence ratio ϕ was varied from small to large values to reach both lean and rich flammability limits.

First, since significant amounts of hydrogen and carbon oxide were documented in most measurements [11,16-18,32-37] of compositions of gases vented out batteries after thermal runaway (with the exception of cases with a low SOC), H_2/CO/air mixtures were simulated by varying the CO:H_2 ratio from 1/9 to 3, i.e., $1/9 \le \alpha \le 3$ in the considered generic fuel blends.

Second, since methane (fuel) and carbon dioxide (inert diluent) were also detected in most measurements [11,16-18,32-37] of compositions of gases vented out batteries after thermal runaway, the aforementioned H_2/CO/air mixtures were extended either by adding extra fuel CH_4 (group 2) or extra diluent CO_2 (group 3). Specifically, $0.058 < \beta < 0.65$ and $\gamma = 0$ in group 2 or $\beta = 0$ and $0.12 < \gamma < 2.7$ in group 3. Large values of γ are associated with a low SOC [11,16-18,32-37].

Third, mixtures listed in Table 2 were studied. All these mixtures are generic, i.e., their compositions differ from measured compositions [11,16-18,32-37] of gases vented out batteries. Alternatively, compositions of gases listed in Table 2 have been designed (i) to cover a range of compositions reported in the cited papers and (ii) to explore the influence of separate variations in concentration of each single species on S_L. Accordingly, mixture compositions listed in Table 2 mimic the measured compositions (e.g., ratios of volume fractions of H_2, CO, and CO_2 are comparable or/and volume fractions of hydrocarbons are comparable), but do not equal to the measured compositions (e.g., hydrocarbons C_nH_m with $n > 1$ or/and $m < 4$ are substituted with CH_4 in Table 2, with investigation of H_2/CO/CO_2/CH_4/C_nH_m blends being the next task for future work), because concentrations of several species are different in each pair of the measured compositions. For convenience, relevant measured mixture compositions are reported for each generic mixture in the right-hand column in Table 2. Here, in the measured case names, numbers show SOC and abbreviations LCO, LFP, NCA, and NMC refer to cathode chemistries, specifically, lithium-cobalt-oxide, lithium-iron-phosphate, lithium-nickel-cobalt-aluminum-oxide, and lithium-manganese-cobalt-oxide, respectively. The reader interested in further details is referred to the cited papers.

In the next section, a small part of computed results is reported to emphasize the key trends and to present apparently surprising observations. Since the same trends were obtained at different unburned gas temperatures, only results computed at $T_u = 300$ K or/and $T_u = 400$ K are presented, whereas data obtained at other T_u, e.g., 500 K or 600 K, will be skipped for brevity. The entire numerical database is available upon request.

---

†Since (i) the adopted software, models, chemical mechanisms, and databases constitute a routine, but still state-of-the-art tool for combustion research and (ii) capabilities of this tool for predicting S_L for various fuel-air mixtures (including all fuels the present work deals with) were already shown by many research groups, computed values of S_L are not compared with experimental data in the present paper for brevity. A large amount of such validation data can be found in a recent review paper by Konnov et al. [22] or, e.g., in Refs. [20,23,52-63].

Table 2
Compositions of generic $H_2/CO/CO_2/CH_4$ mixtures simulated in this work

Number	Species mole fractions				Relevant measured mixture composition
	H_2	CO	CO_2	CH_4	
1	27	27	27	19	LCO 150: $29.6H_2+24.4CO+20.8CO_2+8.2CH_4+17C_nH_m$ [34]
2	29	29	29	13	LCO 100: $27.5H_2+22.7CO+29.8CO_2+6.3CH_4+13.7C_nH_m$ [34]
3	31	31	31	7	LCO/NMC 100: $30H_2+27.6CO+24.9CO_2+8.6CH_4+8.9C_nH_m$ [34]
4	35	25	20	20	Generic Li-ion gas: $34.9H_2+25CO+20.1CO_2+15CH_4+5C_2H_4$ [11]
5	25	45	20	10	NCA 100: $25.7H_2+44.7CO+19.9CO_2+7.1CH_4+2.5C_2H_m$ [35]
6	45	35	10	10	NCA-MJ1c 100: $43.1H_2+37.1CO+9.8CO_2+7CH_4+3C_2H_m$ [32]
7	15	60	20	5	NCA-32Ac 100: $16H_2+58.4CO+20.4CO_2+2.5CH_4+2.7C_2H_m$ [32]
8	35	45	15	5	NCA-32Ec 100: $35.7H_2+44CO+14.5CO_2+3.6CH_4+2.2C_2H_m$ [32]
9	30	5	55	10	LFP 100: $30.9H_2+4.8CO+53.1CO_2+4.1CH_4+7.1C_2H_m$ [34]
10	30	15	45	10	NMC 100: $30.8H_2+13CO+41.2CO_2+6.8CH_4+8.2C_2H_4$ [34]
11	30	15	40	15	NMC 100: $30.8H_2+13CO+41.2CO_2+6.8CH_4+8.2C_2H_4$ [34]
12	20	5	65	10	LFP 50: $20.8H_2+4.8CO+66.2CO_2+1.6CH_4+6.6C_2H_4$ [35]
13	25	40	25	10	NCA 75: $24.3H_2+43.9CO+20.9CO_2+7.5CH_4+3.3C_2H_4$ [32]
14	30	10	50	10	LFP 100: $29.4H_2+9.1CO+48.3CO_2+5.4CH_4+7.7C_2H_m$ [35]
15	30	5	30	35	LCO 50: $30.7H_2+3.6CO+32CO_2+5.7CH_4+28C_nH_m$ [33]
16	25	30	35	10	NMC 100: $22.4H_2+28.9CO+36.8CO_2+5.2CH_4+6.6C_2H_m$ [34]
17	17.5	40	32.5	10	NCA 50: $17.5H_2+39.9CO+33.8CO_2+5.2CH_4+3.6C_2H_m$ [35]
18	15	5	65	15	NCA 25: $15.5H_2+5.5CO+62.8CO_2+8.7CH_4+7.5C_2H_4$ [35]

4. Results and discussion

4.1. H_2/CO/air mixtures

Figure 1 reports dependencies of S_L on the equivalence ratio ϕ, computed for three different $\alpha = 1/9$, 1, and 3, see curves plotted in dashed, solid, and dotted-dashed lines, respectively, using GRI [23], Princeton [24], and San Diego [25] chemical mechanisms, see curves plotted in blue, black, and red lines, respectively. Two observations are worth noting.

First, while all three mechanisms yield sufficiently close results, there are some differences, which are more pronounced in richer mixtures, i.e., at larger ϕ. Specifically, values of S_L computed using Princeton mechanism [24] at large ϕ and large α (i.e., 25% H_2) are higher when compared to two other mechanisms and values of S_L computed using GRI mechanism [23] at large ϕ and small α (i.e., 90% H_2) are smaller when compared to two other mechanisms. The fact that GRI mechanism is not the best one for hydrogen flames is well known [22,57]. Nevertheless, small quantitative differences between $S_L(\phi)$-curves computed using the three mechanisms (such differences are also small for other studied mixtures, not shown for brevity) justify adopting any of them in a qualitative study. Results presented in the following were obtained using Princeton mechanism [24] if another mechanism is not specified. From the numerical perspective, this mechanism is more robust, i.e. a wider range of ϕ can be scanned using code PREMIX software package [29] without numerical failures.

Second, an increase in the volume fraction of CO results in decreasing S_L (and increasing δ_L, not shown for brevity). Such a trend is expected, because both hydrogen reactivity and hydrogen diffusivity are higher when compared to CO. However, this trend is difficult to see near lean flammability limit in Fig. 1, because S_L is very small in lean mixtures when compared to the peak $S_L(\phi)$ in moderately rich ones.

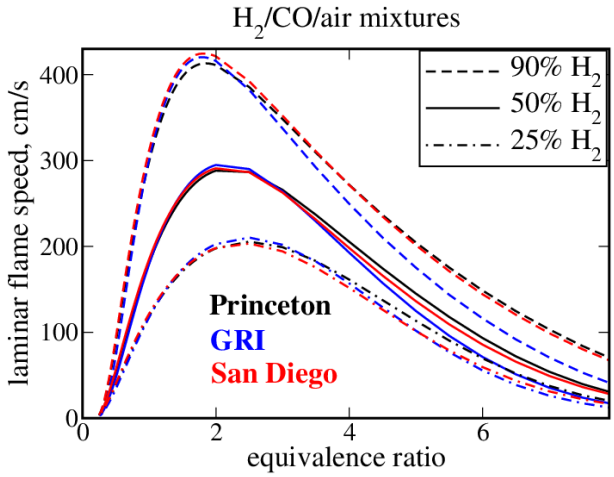

Figure 1: Speeds of H_2/CO/air laminar flames computed using GRI [23], Princeton [24], and San Diego [25] chemical mechanisms vs. equivalence ratio under room conditions. Volume percentage of hydrogen in H_2-CO fuel blend is specified in legends. $T_u = 400$ K, $P = 1$ atm.

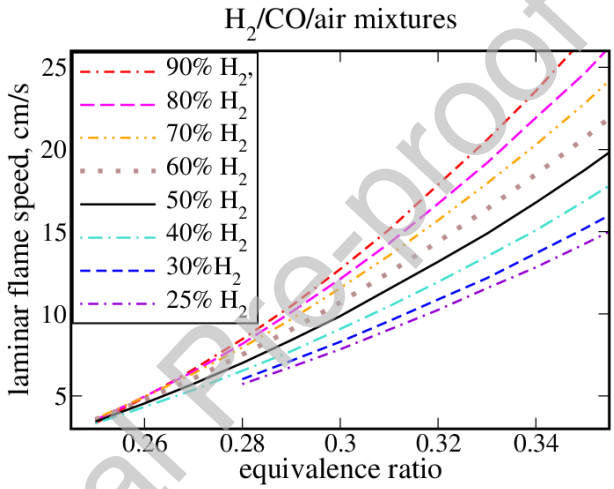

Figure 2: Laminar flame speeds of lean H_2/CO/air mixtures computed for various volume fractions of hydrogen in fuel blends, specified in legends, using Princeton chemical mechanism [24]. $T_u = 400$ K, $P = 1$ atm.

Accordingly, Fig. 2 zooms dependencies of S_L on the equivalence ratio, computed for various α at small values of ϕ. These results show that an increase in α by a factor of 27 (i.e., from 1/9 to 3) results in weakly decreasing $S_L(\phi)$. For instance, the difference in values of equivalence ratio associated with $S_L = 6$ cm/s is smaller than 0.02 for $\alpha = 1/9$ and $\alpha = 3$, cf. curves plotted red dotted-double-dashed and violet dotted-dashed lines, respectively. The same trend is observed in Fig. 3.

Figure 3 also shows that GRI mechanism yields substantially larger values of ϕ^* associated with $S_L(\phi) = 5$ cm/s, see blue triangles, when compared to two other mechanisms. In other words, GRI mechanism tends to result in larger ϕ associated with lean flammability limit.

All in all, Figs. 1-3 indicate that an increase in volume fraction of carbon oxide in H_2/CO blend results in decreasing $S_L(\phi)$, with this trend being weakly pronounced at low equivalence ratios. Accordingly, an increase in α weakly affects lean flammability limit, especially at $\alpha < 1$ (curves in Fig. 3 look saturated at large volume fractions of hydrogen).

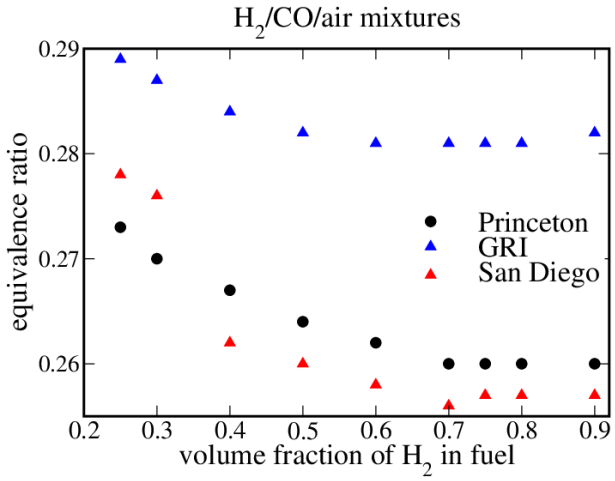

Figure 3: Equivalence ratios associated with $S_L(\phi^*) = 5$ cm/s vs. volume percentage of hydrogen in H_2/CO fuel blends. Results computed using GRI [23], Princeton [24], and San Diego [25] chemical mechanisms are plotted in blue triangles, black cercles, and red triangles, respectively. $T_u = 400$ K, $P = 1$ atm.

4.2. H_2/CO/CO_2/air and H_2/CO/CH_4/air mixtures

Figures 4a and 4b report dependencies of S_L on the equivalence ratio ϕ, computed for (a) H_2/CO/CO_2/air and (b) H_2/CO/CH_4/air mixtures using Princeton chemical mechanism [24] at $T_u = 400$ K. Here, results for a single set of mixtures ($\alpha = 3$) are presented, because similar trends are observed for other α and for other T_u (not shown for brevity). To place the focus of discussion on lean mixtures, the plotted results are restricted to $\phi < 0.45$.

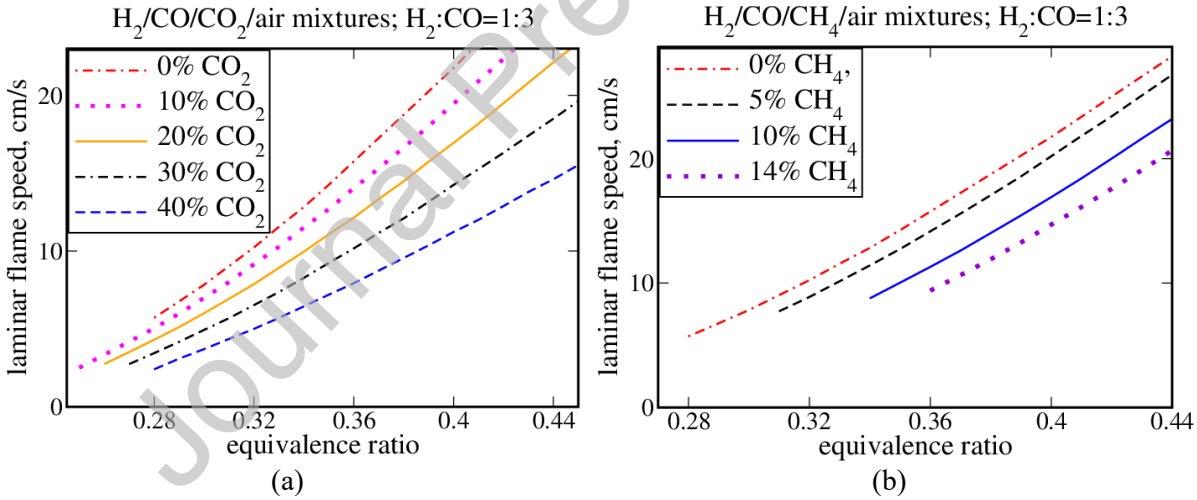

Figure 4: Laminar flame speeds of lean (a) H_2/CO/CO_2/air and (b) H_2/CO/CH_4/air mixtures computed for various volume fractions of CO_2 and CH_4, respectively, in fuel blends, with ratio of H_2 and CO volume fractions being equal to 1:3. Princeton chemical mechanism [24]. $T_u = 400$ K, $P = 1$ atm.

Three observations are worth noting. First, as expected, addition of either CO_2 or CH_4 to an H_2/CO fuel blend results in decreasing S_L. Second, the influence of carbon dioxide on $S_L(\phi)$ is quite moderate in lean mixtures, see Fig. 4a. For instance, the addition of 40% CO_2 to the considered H_2/CO fuel blend results in increasing ϕ^* associated with $S_L(\phi) = 5$ cm/s from 0.28 to 0.32, cf. curves plotted in red dotted-dashed and blue dashed lines in Fig. 4a (from 0.29 or 0.27 to 0.34 or 0.31, respectively, using GRI [23] or San Diego [25] mechanism, respectively). Accordingly, the risk of fires could be significant even if gases vented out a battery contain a large amount of carbon dioxide, e.g., in case of a low SOC.

The computed weak influence of CO_2 on $S_L(\phi)$ in lean mixtures is associated with a small amount of the added CO_2 when compared to N_2 in the air. Indeed, even if an H_2/CO/CO_2 fuel blend contains 40% CO_2, the mole fraction of CO_2 in the entire fuel-air mixture is much smaller than the mole fraction

of N_2, e.g., a ratio of X_{CO_2} and X_{N_2} is about 0.1 if $\phi = 0.3$ and $\alpha = X_{CO}/X_{H_2} = 3$. Consequently, even sufficiently large volume fractions of CO_2 in gases vented out a battery with a low SOC do not guarantee low fire risks.

Third, if one compares the influence of the addition of (i) CO to H_2, see Fig. 3, (ii) CO_2 to H_2/CO fuel blend, see Fig. 4a, and (iii) CH_4 to H_2/CO fuel blend, see Fig. 4b, the effect magnitude is the lowest in case (i) and the highest in case (iii). Thus, while carbon dioxide and methane are an inert diluent and a fuel, respectively, a decrease in $S_L(\phi)$ is smaller when CO_2 is added. For example, the addition of 14% CH_4 results in increasing ϕ associated with $S_L(\phi) = 10$ cm/s more (from 0.32 to 0.37, cf. curves plotted in red dotted-dashed and violet dotted lines in Fig. 4b) when the addition of 30% CO_2 (from 0.32 to 0.36, cf. curves plotted in red dotted-dashed and black dotted-double-dashed lines in Fig. 4a). GRI [23] or San Diego [25] mechanism yields the same trend, e.g., $\Delta\phi = 0.05$ or 0.04 respectively, in the former case (14% CH_4) and $\Delta\phi = 0.03$ for both mechanisms in the latter case (30% CO_2).

To explain these apparently surprising numerical data, let's compare mole fractions on inert diluents in lean H_2/CO/air, H_2/CO/CO_2/air, and H_2/CO/CH_4/air mixtures. Formulas collected in Table 1 show that X_{in} does not depend on α in H_2/CO/air mixtures, i.e., blending of hydrogen with carbon oxide does not increase X_{in}. This explains sufficiently close values of $S_L(\phi)$ obtained at low ϕ from H_2/CO/air mixtures characterized by significantly different α. At larger equivalence ratios, contribution of hydrogen to heat diffusivity of the mixture is greater, resulting in increasing the heat diffusivity and, hence, increasing S_L with decreasing α.

For H_2/CO/CO_2/air or H_2/CO/CH_4/air mixture, an increase in γ or β, respectively, results in increasing X_{in}, as expected and in line with Fig. 4. Moreover, after some algebra, the difference between mole fractions of inert diluents in the two sets of flames (i.e., CO_2, unburned O_2, and N_2 in the former set or unburned O_2 and N_2 in the latter set), evaluated at the same ϕ, is equal to

$$X_{in}(\beta = 0) - X_{in}(\gamma = 0) = \frac{-7.14\phi(1+\alpha)\beta + 1.5\phi^2(1+\alpha)(\beta+\gamma) + 3\beta\gamma\phi^2}{\left[\phi(1+\alpha+\gamma) + 4.76\left(\frac{1}{2}+\frac{\alpha}{2}\right)\right]\left[\phi(1+\alpha+\beta) + 4.76\left(\frac{1}{2}+\frac{\alpha}{2}+2\beta\right)\right]}. \quad (3)$$

This difference is expected to be negative at comparable β and γ and a small ϕ due to the term $-7.14\phi(1+\alpha)\beta$, which is linear with respect to ϕ, whereas the two other terms in the nominator are proportional to much smaller ϕ^2. Therefore, in lean reactant-air mixtures characterized by the same equivalence ratio, an increase in the mole fraction of inert diluents due to the addition of one mole of methane to an H_2/CO blend is significantly larger when compared to the counterpart increase in X_{in} due to the addition of one mole of carbon dioxide to the same blend. Accordingly, a decrease in $S_L(\phi)$ is more pronounced in the former case, as shown in Fig. 4.

In addition, for instance in blends $0.81H_2$+0.09CO+$0.1CH_4$ and $0.81H_2$+0.09CO+$0.1CO_2$, the laminar flame speeds $S_L(T_u = 400\ \text{K})$ are equal to 25.8 and 42.4 cm/s, respectively, provided that the same equivalence ratio $\phi = 0.40$ is retained. The differences computed using GRI [23] and San Diego [25] mechanisms are equal to 16.9 and 11.1 cm/s, respectively. Thus, the addition of a fuel (CH_4) to an H_2/CO blend may result in decreasing $S_L(\phi)$ when compared to the addition of the same amount (per unit hydrogen volume) of a diluent (CO_2) to the same blend. From this perspective, methane may mitigate fire better than carbon dioxide.

It is worth stressing, however, that such an apparently surprising trend is solely observed if the same equivalence ratio is retained. On the contrary, if CH_4 is simply substituted with CO_2, both ϕ and, hence, S_L are decreased. For example, if $\phi = 0.40$ for the blend $0.81H_2$+0.09CO+$0.1CH_4$, simple substitution of methane with carbon dioxide yields $\phi = 0.28$ and $S_L(T_u = 400\ \text{K}, \phi = 0.28) = 8.9$ cm/s, i.e., a decrease by a factor of about three when compared to the former (H_2/CO/CH_4/air) flame.

It is also of interest to note that the next-to-the-bottom row in Table 1 shows opposite dependencies of X_{in} on α and β. Specifically, X_{in} is decreased when β is decreased or α is increased. Thus, an increase in the ratio of the volume fractions of carbon oxide and hydrogen in H_2/CO/CH_4 blend may result in decreasing mole fraction of inert diluents in the mixture (if the equivalence ratio retains its value). Accordingly, contrary to a decrease in S_L with increasing α in H_2/CO/air mixtures, discussed in Sect. 4.1, $S_L(\phi)$ may increase with increasing α in H_2/CO/CH_4 blends. Indeed, the present simulations show

that such an apparently surprising trend can be observed, e.g., see Table 3, which reports typical characteristics of lean H_2/CO/CH_4/air flames, computed by varying the volume ratio of CO and H_2, i.e., α, and retaining the same ϕ and the same volume ratio of CH_4 and H_2, i.e., β. All three chemical mechanisms predict this trend, i.e., an increase in S_L by α if ϕ and β retain their values. Similar results were obtained at other low equivalence ratios and other unburned gas temperatures.

Table 3
Characteristics of lean H_2/CO/CH_4/air and H_2/CO/CO_2/air flames with different volume fractions of CO

Fuel blend	β	γ	ϕ	T_u, K	α	X_{in}	T_{ad}, K	S_L, cm/s		
								[24]	[23]	[25]
H_2/CO/CH_4	0.5	0	0.42	400	0.5	0.8282	1487	13.7	14.4	17.2
					1.0	0.8212	1562	15.9	15.5	18.7
					1.83	0.8128	1581	18.1	16.7	20.2
					3.50	0.8028	1604	19.8	17.5	21.3
H_2/CO/CO_2	0	0.5	0.42	400	0.5	0.7857	1502	29.6	22.4	30.5
					1.0	0.7831	1544	26.7	21.8	28.3
					1.83	0.7808	1578	24.5	20.5	26.0
					3.50	0.7787	1612	21.8	18.8	23.2

Besides, the bottom row in Table 1 shows opposite dependencies of X_{in} on α and γ for H_2/CO/CO_2 blends, i.e., X_{in} is decreased when γ is decreased or α is increased. Table 3 confirms this trend and shows that X_{in} is decreased and T_{ad} is increased with increasing α in H_2/CO/CO_2 blends, provided that ϕ and γ retain their values. However, for these fuel blends, such an increase in the combustion temperature with decreasing mole fraction of H_2 may be counterbalanced by decreasing molecular fuel and heat diffusivities and decreasing reactivity, which is higher for hydrogen. Table 3 implies that the latter effects dominate the increase in T_{ad} and results in decreasing S_L with increasing the volume ratio of CO, in line with common expectations. Thus, while the mole fraction of inert diluents plays an important role, other factors such as molecular transport coefficients should also be considered.

Nevertheless, the important role played by X_{in} can be further illustrated by comparing characteristics of lean H_2/CO/CH_4/air and H_2/CO/CO_2/air flames, reported in Table 3. At the same ϕ, the same T_u, the same α, and $\beta = \gamma$, the latter mixtures, which contain an extra inert diluent, i.e., CO_2, are characterized by smaller X_{in}, higher T_{ad}, and higher S_L despite the former blends contain an extra fuel, i.e., CH_4.

4.3. H_2/CO/CO_2/CH_4/air mixtures

Figures 5a and 5b report maximum (over various ϕ) laminar flame speeds and minimum laminar flame thicknesses, respectively. These data have been computed using Princeton chemical mechanism [24] and varying the equivalence ratio for 18 mixtures listed in Table 2. The data are plotted vs. mole fraction of carbon dioxide in each generic H_2/CO/CO_2/CH_4 blend. These mole fractions are specified in the fourth column in Table 2. Black circles and red squares show S_L or δ_L computed at $T_u = 300$ K and 400 K, respectively. As expected, variations in the flame speed and thickness show opposite trends, because δ_L is inversely proportional to S_L in a typical premixed flame.

Figure 5 shows a significant decrease (increase) in the maximum (minimum, respectively) values of S_L (δ_L, respectively) with increasing mole fraction of CO_2 in fuel blends. However, these extreme values are reached in near-stoichiometric mixtures, contrary to lean mixtures discussed in the previous section.

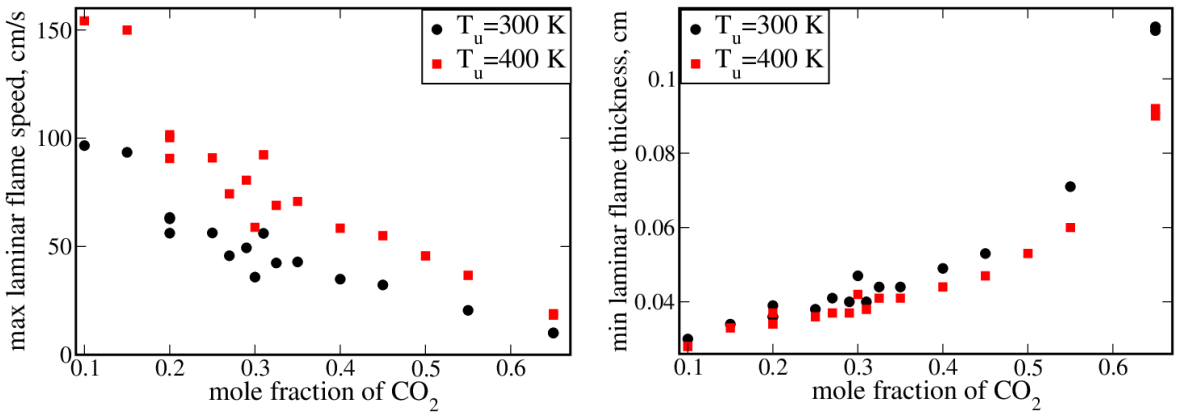

Figure 5: (a) Maximum laminar flame speeds and (b) minimum laminar flame thicknesses for fuel blends listed in Table 2. These extreme values have been obtained by varying equivalence ratio for each single blend and are plotted vs. mole fraction of CO_2 in that fuel blend. Black circles and red squares show results computed at $T_u = 300$ K and $T_u = 400$ K, respectively. Princeton chemical mechanism [24]. $P = 1$ atm.

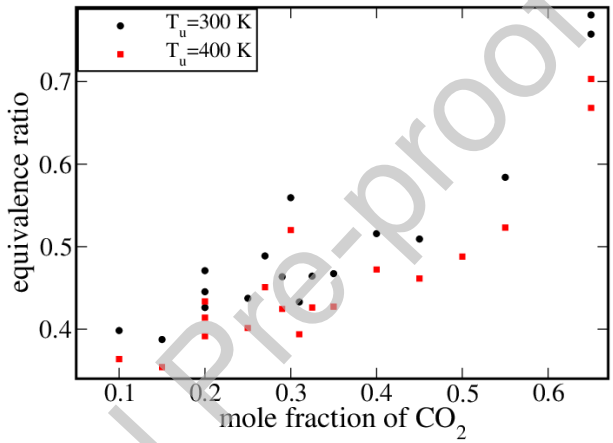

Figure 6: Equivalence ratios associated with $S_L = 12$ cm/s, computed for various fuel blends listed in Table 2. These results are plotted vs. mole fraction of CO_2 in fuel blend, reported in the fourth column in Table 2. Black circles and red squares show results computed at $T_u = 300$ K and $T_u = 400$ K, respectively. Princeton chemical mechanism [24]. $P = 1$ atm.

The lean burning of the fuel blends considered is addressed in Fig. 6, which reports equivalence ratios ϕ associated with a small laminar flame speed of $S_L = 12$ cm/s. This laminar flame speed does not characterize lean flammability limit but is chosen to illustrate the trend, i.e., weak influence of X_{CO_2} on $S_L(\phi)$, using another value of S_L that differs from values adopted in the previous examples. The results are plotted vs. mole fraction X_{CO_2} of CO_2 in a generic fuel blend. Black circles and red squares show data computed at $T_u = 300$ K and $T_u = 400$ K, respectively. While the trend of increasing ϕ with increasing X_{CO_2} is well pronounced, the effect magnitude is quite moderate. With the exception of cases 12 and 18, characterized by X_{CO_2} as large as 0.65, the other 16 mixtures are characterized by significant laminar flame speeds at ϕ as low as 0.5 ($T_u = 400$ K) or lower. Even in the two other cases (12 and 18 in Table 2), $S_L = 12$ cm/s is reached at ϕ smaller than 0.7 at $T_u = 400$ K. These numerical results again indicate that a large volume fraction of carbon dioxide in gases vented out a battery after thermal runaway does not exclude fire risks. At $T_u = 400$ K, the lean flammability limit associated with $S_L(\phi^*) = 5$ cm/s is well below $\phi = 0.7$ even if mole fraction of CO_2 in a fuel blend is as large as 0.65. Specifically, for mixtures 12 and 18 in Table 2, $S_L = 5$ cm/s at $\phi = 0.53$ and 0.55, respectively, if $T_u = 400$ K. Thus, a low SOC does not guarantee the lack of fire risk.

5. Conclusions

Complex-chemistry simulations of unperturbed laminar premixed flames were performed for a wide range of $H_2/CO/CO_2/CH_4$ blends and equivalence ratios at four different temperatures of unburned reactants. Three different state-of-the-art chemical mechanisms and multicomponent diffusion model with Soret effect were adopted. The focus of the present analysis was placed on the influence of concentrations of CO, CO_2, and CH_4 on the computed laminar flame speeds and a surrogate of lean flammability limit, i.e., equivalence ratio ϕ^* associated with a small laminar flame speed, i.e., $S_L(\phi^*) = 5$ cm/s.

As expected, the results show a decrease in S_L and an increase in ϕ^* with decreasing hydrogen mole fraction in the reactants. However, the following three trends are apparently surprising. First, both $S_L(\phi)$ in lean mixtures and, especially, ϕ^* depend weakly on mole fraction of CO in H_2/CO fuel blends. Second, a decrease in $S_L(\phi)$ in lean mixtures is more (less) pronounced when adding CH_4 (CO_2, respectively) to H_2/CO fuel blends. Accordingly, under certain conditions, fuel (CH_4) can mitigate fire risk more efficiently than diluent (CO_2) provided that the equivalence ratio retains the same value. Third, an increase in a ratio of mole fractions of carbon oxide and hydrogen in lean $H_2/CO/CH_4$/air mixtures characterized by the same equivalence ratio may result in increasing $S_L(\phi)$.

All these observations are attributed to a larger (smaller) increase in the mole fraction of inert components when adding CH_4 (CO_2, respectively) to H_2/CO fuel blends (provided that the equivalence ratio retains the same value). Nevertheless, other factors such as high diffusivity and high reactivity of hydrogen can also play an important role and, e.g., control a decrease in $S_L(\phi)$ with increasing volume ratio of carbon oxide and hydrogen in lean $H_2/CO/CO_2$/air mixtures.

Finally, the computed results also show that even a large volume fraction of carbon dioxide, e.g., 65%, in gases vented out a battery after thermal runaway does not exclude fire risks.

CRediT authorship contribution statement

A.N. Lipatnikov: Conceptualization, Methodology, Formal analysis, Writing – original draft, Writing – review & editing, Supervision, Funding acquisition.

Declaration of competing interest

The authors declare that they have no known competing financial interests or personal relationships that could have appeared to influence the work reported in this paper.

Acknowledgment

This work was supported by Area of Advance Energy at Chalmers University of Technology, project number 304 13 024.

References

[1] M.S. Whittingham, Science **192**, 1126 (1976).
[2] J.M. Tarascon and M. Armand, Nature **414**, 359 (2001).
[3] S. Pacala and R. Socolow, Science **305**, 968 (2004).
[4] A.F. Blum and R.T. Long Jr., *Fire hazard assessment of lithium ion battery energy storage systems* (Springer New York, 2016).
[5] M. Ghiji, V. Novozhilov, K. Moinuddin, P. Joseph, I. Burch, B. Suendermann, and G. Gamble, Energies **13**, 5117 (2020).
[6] S. Abada, G. Marlair, A. Lecocq, M. Petit, V. Sauvant-Moynot, and F. Huet, J. Power Sources **306**, 178 (2016).
[7] L. Kong, C. Li, J. Jiang, and M. Pecht, Energies **11**, 2191 (2018).
[8] X. Feng, M. Ouyang, X. Liu, L. Lu, Y. Xia, and X. He, Energy Storage Mater. **10**, 246 (2018).
[9] Y. Zheng, Y. Che, X. Hu, X. Sui, D.-I. Stroe, and R. Teodorescu, Prog. Energy Combust. Sci. **100**, 101120 (2024).
[10] Q. Wang, B. Mao, S.I. Stoliarov, and J. Sun, Prog. Energy Combust. Sci. **73**, 95 (2019).

[11] M. Henriksen, K. Vaagsaether, J. Lundberg, S. Forseth, and D. Bjerketvedt, Fire Safety J. **126**, 103478 (2021).
[12] A. Cellier, F. Duchaine, T. Poinsot, G. Okyay, M. Leyko, and M. Pallud, Combust. Flame **250**, 112648 (2023).
[13] T. Atherley, S. de Persis, N. Chaumeix, Y. Fernandes, A. Bry, A. Comandini, O. Mathieu, S. Alturaifi, C.R. Mulvihill, and E.L. Petersen, Proc. Combust. Inst. **38**, 977 (2021).
[14] K. Kanayama, S. Takahashi, S. Morikura, H. Nakamura, T. Tezuka, and K. Maruta, Combust. Flame **237**, 111810 (2022).
[15] R. Yu, J. Liu, W. Liang, Y. Wu, C. Tang, H. Wang, and M. Ouyang, Combust. Flame **246**, 112465 (2022).
[16] Y. Fernandes, A. Bry, and S. de Persis, J. Power Sources **389**, 106 (2018).
[17] A.R. Baird, E.J. Archibald, K.C. Marr, and O.A. Ezekoy, J. Power Sources **446**, 227257 (2020).
[18] S. Chen, Z. Wang, J. Wang, X. Tong, and W. Yan, J. Loss Prevent. Process. Ind. **63**, 103992 (2020).
[19] R. Yu, J. Liu, W. Liang, C.K. Law, H. Wang, and M. Ouyang, Proc. Combust. Inst. **39**, 3031 (2023).
[20] M. Henriksen, K. Vaagsaether, J. Lundberg, S. Forseth, and D. Bjerketvedt, J. Power Sources **506**, 230141 (2021).
[21] R. Yu, J. Liu, W. Liang, C.K. Law, H. Wang, and M. Ouyang, Combust. Flame **249**, 112631 (2023).
[22] A.A. Konnov, A. Mohammad, V.R. Kishore, N. Kim, C. Prathap, and S. Kumar, Prog. Energy Combust. Sci. **68**, 197 (2018).
[23] G.P. Smith, D.M. Golden, M. Frenklach, N.W. Moriarty, B. Eiteneer, M. Goldenberg, C.T. Bowman, R.K. Hanson, S. Song, W.C.G. Jr, V.V. Lissianski, and Z. Qin, GRI-MECH 3.0. http://combustion.berkeley.edu/gri-mech/version30/text30.html#cite, 1999 (accessed 5 August 2025).
[24] J. Li, Z. Zhao, A. Kazakov, and F.L. Dryer, Int. J. Chem. Kinetics **39**, 109 (2007).
[25] The San Diego mechanism, Chemical-kinetic mechanisms for combustion applications, http://web.eng.ucsd.edu/mae/groups/combustion/mechanism.html, 2016 (accessed 5 August 2025).
[26] R.J. Kee, F.M. Rupley, and J.A. Miller, CHEMKIN-II: A FORTRAN chemical kinetics package for the analysis of gas-phase chemical kinetics, Report No. SAND-89-8009, Sandia National Laboratories, 1989.
[27] R.J. Kee, F.M. Rupley, J.A. Miller, M.E. Coltrin, J.F. Grcar, E. Meeks, H.K. Moffat, A.E. Lutz, G. Dixon-Lewis, M.D. Smooke, J. Warnatz, G.H. Evans, R.S. Larson, R.E. Mitchell, L.R. Petzold, W.C. Reynolds, M. Caracotsios, W.E. Stewart, P. Glarborg, C. Wang, and O. Adigun, CHEMKIN Collection, Release 3.6, Reaction Design, Inc., San Diego, CA, 2000.
[28] D.G. Goodwin, H.K. Moffat, and R.L. Speth, Cantera: an object-oriented software toolkit for chemical kinetics, thermodynamics, and transport processes, Version 2.3.0, https://doi.org/10.5281/zenodo.170284, 2017 (accessed 5 August 2025).
[29] R.J. Kee, J.F. Crcar, M.D. Smooke, and J.A. Miller, PREMIX: A FORTRAN program for modeling steady laminar one-dimensional premixed flames, Report No. SAND-85-8240, Sandia National Laboratories, 1985.
[30] R.J. Kee, G. Dixon-Lewis, J. Warnatz, M.E. Coltrin, and J.A. Miller, A FORTRAN computer code package for the evaluation of gas-phase multicomponent transport properties, Report No. SAND86-8246, Sandia National Laboratories, 1986.
[31] A.W. Jasper and J.A. Miller, Combust. Flame **161**, 101 (2014).
[32] M. Lammer, A. Königseder, and V. Hacker, RSC Adv. **7**, 24425 (2017),
[33] V. Somandepalli, K. Marr, and Q. Horn, SAE Int. J. Altern. Powertrains. **3**, 98 (2014).
[34] A.W. Golubkov, D. Fuchs, J. Wagner, H. Wiltsche, C. Stangl, G. Fauler, G. Voitic, A. Thaler, and V. Hacker, RSC Adv. **4**, 3633 (2014).
[35] A.W. Golubkov, S. Scheikl, R. Planteu, G. Voitic, H. Wiltsche, C. Stangl, G. Fauler, A. Thaler, and V. Hacker, RSC Adv. **5**, 57171 (2015).
[36] S. Koch, A. Fill, and K.P. Birke, J. Power Sources **398**, 106 (2018).
[37] T. Maloney, Lithium battery thermal runaway vent gas analysis, Technical Report, Federal Aviation Administration, Office of Hazardous Materials Safety, 2016.
[38] Y.B. Zeldovich, G.I. Barenblatt, V.B. Librovich, and G.M. Makhviladze, *The mathematical theory of combustion and explosions* (Consultants Bureau New York, 1985).
[39] T. Poinsot and D. Veynante, *Theoretical and numerical combustion*, second ed. (Edwards Philadelphia, 2005).

[40] A.N. Lipatnikov, Prog. Energy Combust. Sci. **62**, 87 (2017).
[41] A.N. Lipatnikov and J. Chomiak, Prog. Energy Combust. Sci. **28**, 1 (2002).
[42] B. Lewis and G. von Elbe, *Combustion, flames and explosions of gases*, second ed. (Academic Press New York, 1961).
[43] J. Buckmaster, P. Clavin, A. Liñán, M. Matalon, N. Peters, G. Sivashinsky, and F.A. Williams, Proc. Combust. Inst. **30**, 1 (2005).
[44] J. Jarosinski, Prog. Energy Combust. Sci. **12**, 81 (1986).
[45] W.J. Pitz, C.K. Westbrook, Chemical kinetic modeling of hydrogen combustion limits, Report No. LLNL-TR-402715, Lawrence Livermore National Laboratory, 2008.
[46] A. Z. Mendiburu, J.A. Carvalho Jr., and Y. Ju, Energy Fuels **37**, 4151 (2023).
[47] F. Van den Schoor, R.T.E. Hermanns, J.A. van Oijen, F. Verplaetsen, and L.P.H. de Goey, J. Hazard. Mater. **150**, 573 (2008).
[48] J.F. Grcar, J.B. Bell, and M.S. Day, Proc. Combust. Inst. **32**, 1173 (2009).
[49] W. Liang, Z. Chen, F. Yang, and H. Zhang, Proc. Combust. Inst. **34**, 695 (2013).
[50] Z. Zhou, F.E. Hernández-Pérez, Y. Shoshin, J.A. van Oijen, and L.P.H. de Goey, Combust. Theory Modell. **21**, 879 (2017).
[51] E. Ranzi, A. Frassoldati, R. Grana, A. Cuoci, T. Faravelli, A.P. Kelley, and C.K. Law, Prog. Energy Combust. Sci. **38**, 468 (2012).
[52] A.L. Sánchez and F.A. Williams, Prog. Energy. Combust. Sci. **41**, 1 (2014).
[53] H.J. Curran, Proc. Combust. Inst. **37**, 57 (2019).
[54] J. Natarajan, T. Lieuwen, and J. Seitzman, Combust. Flame **151**, 104 (2007).
[55] M. Akram, P. Saxen, and S. Kumar, Energy Fuels **27**, 3460 (2013).
[56] D. Lapalme and P. Seers, Int. J. Hydrogen Energy **39**, 3477 (2014).
[57] C. Olm, I.Gy. Zsély, R. Pálvölgyi, T. Varga, T. Nagy, H.J. Curran, and T. Turányi, Combust. Flame **161**, 2219 (2014).
[58] H. Sun, S.I. Yang, G. Jomaas, and C.K. Law, Proc. Combust. Inst. **31**, 439 (2007).
[59] N. Bouvet, C. Chauveau, I. Gökalp, and F. Halter, Proc. Combust. Inst. **33**, 913 (2011).
[60] H.J. Burbano, J. Pareja, and A.A. Amell, Int. J. Hydrogen Energy **36**, 3232 (2011).
[61] Y. Zhang, W. Shen, M. Fan, H. Zhang, and S. Li, Combust. Flame **161**, 2492 (2014).
[62] Q. Zhou, C.S. Cheung, C.W. Leung, X. Lib, X. Li, and Z. Huang, Fuel **238**, 149 (2019).
[63] P. Saxena and F.A. Williams, Combust. Flame **145**, 316 (2006).
[64] Z. Wang, X. Li, T. Li, A. Dreizler, S.M. Mousavi, A.N. Lipatnikov, and B. Zhou, Combust. Flame, **275**, 114054 (2025).
[65] N. Peters, *Turbulent combustion* (Cambridge University Press Cambridge UK, 2000).
[66] A.N. Lipatnikov, *Fundamentals of premixed turbulent combustion* (CRC Press Florida, 2012).

Declaration of competing interest

The authors declare that they have no known competing financial interests or personal relationships that could have appeared to influence the work reported in this paper.